Glycobiology vol. 23 no. 6 pp. 654–663, 2013
doi:10.1093/glycob/cwt006
Advance Access publication on February 19, 2013

Inhibition of galectin-3 reduces atherosclerosis in apolipoprotein E-deficient mice

Alison C MacKinnon[2,†], Xiaojun Liu[3,†], Patrick WF Hadoke[4], Mark R Miller[4], David E Newby[4], and Tariq Sethi[1,5]

[2]Scottish Centre for Regenerative Medicine, SCRM Building, University of Edinburgh, Edinburgh Bioquarter, 5 Little France Drive, Edinburgh EH16 4UU, UK; [3]College of Animal Science & Technology, Shihezi University, Shihezi 8320003, Xinjiang, China; [4]Centre for Cardiovascular Science, The Queen's Medical Research Institute, University of Edinburgh, 47 Little France Crescent, Edinburgh EH16 4TJ, UK; and [5]Department of Respiratory Medicine and Allergy, King's College Denmark Hill Campus, Bessemer Road, London SE5 9RJ, UK

Received on October 29, 2012; revised on January 13, 2013; accepted on January 20, 2013

Atherosclerosis is a major risk factor for cardiovascular disease (CVD) and stroke. Galectin-3 is a carbohydrate-binding lectin implicated in the pathophysiology of CVD and is highly expressed within atherosclerotic lesions in mice and humans. The object of this present study was to use genetic deletion and pharmacological inhibition in a well-characterized mouse model of atherosclerosis to determine the role of galectin-3 in plaque development. Apolipoprotein-E/galectin-3 knockout mice were generated and fed a high-cholesterol "western" diet. Galectin-3 deletion had no consistent effect on the serum lipid profile but halved atherosclerotic lesion formation in the thoracic aorta (57% reduction), the aortic arch (50% reduction) and the brachiocephalic arteries. The aortic plaques were smaller, with reduced lipid core and less collagen. In apolipoprotein E-deficient ($ApoE^{-/-}$) mice, there was a switch from high inducible nitric oxide expression in early lesions (6 weeks) to arginase-1 expression in later lesions (20 weeks), which was reversed in $ApoE^{-/-}$/gal-$3^{-/-}$ mice. Administration of modified citrus pectin, an inhibitor of galectin-3, during the latter stage of the disease reduced plaque volume. We conclude that inhibiting galectin-3 causes decreased atherosclerosis. Strategies to inhibit galectin-3 function may reduce plaque progression and potentially represent a novel therapeutic strategy in the treatment of atherosclerotic disease.

Keywords: atherosclerosis / galectin-3 / inflammation / macrophages / plaque

Introduction

Atherosclerosis is a major cause of cardiovascular disease (CVD) and stroke. In the United States it has been estimated that there are ~2000 deaths from CVD every day, more every year than from cancer, respiratory disease and accidents combined (Roger et al. 2011). Atherosclerosis is recognized as being a chronic inflammatory disease (Hansson et al. 2006). Macrophages recruited to the vascular intima engulf lipoprotein particles, such as modified low-density lipoprotein (LDL) cholesterol and differentiate into foam cells, which orchestrate lesion development by promoting inflammation, smooth muscle cell proliferation and extracellular matrix deposition.

Galectin-3, also known as Mac-2 antigen, is a 26 kDa β-galactoside-binding protein that participates in a variety of biological processes, including phagocytosis (Dumic et al. 2006), cell growth and proliferation (Dong and Hughes 1997), adhesion (Nakahara et al. 2005) and apoptosis (Maeda et al. 2004). It is highly expressed by macrophages, is upregulated in chronic inflammatory conditions and plays a fundamental role in macrophage activation and function (Arar et al. 1998; Nachtigal et al. 1998; Henderson et al. 2006; MacKinnon et al. 2008). We have previously shown that mice deficient in galectin-3 have a specific defect in alternative (M2) macrophage activation and exhibit "scarless" repair despite chronic insult in several organ systems (Henderson et al. 2006; MacKinnon et al. 2008).

Galectin-3 has an important role in the development of CVD. It has been implicated in cardiac fibrosis and remodeling, is increased in models of heart failure (Sharma et al. 2004) and has prognostic value in heart failure patients (Ho et al. 2012) and is a predictor of response to statin therapy in heart failure (Gullestad et al. 2012). Furthermore, a high circulating galectin-3 level predicts major adverse clinical outcomes following acute myocardial infarction (Tsai et al. 2012). In a study of 7968 patients aimed to correlate circulating galectin-3 with cardiovascular risk factors showed that galectin-3 predicts all-cause mortality in the general population (de Boer et al. 2012).

Galectin-3 is highly expressed in macrophages within human atherosclerotic plaques and in murine models of atheroma (Arar et al. 1998; Nachtigal et al. 1998). In the present study, we investigate the role of galectin-3 in a well-characterized murine model of atherosclerosis; high-cholesterol feeding in apolipoprotein E-deficient ($ApoE^{-/-}$) C57/B6 mice. We show that mice deficient in galectin-3 show

[1]To whom correspondence should be addressed: Tel: +44-203-299-3165; Fax: +44-203-299-3791; e-mail tariq.sethi@kcl.ac.uk
[†]These authors contributed equally.

reduced plaque volume and reduced M2 activation of plaque macrophages. Moreover, we show that modified citrus pectin, an orally active inhibitor of galectin-3, reduces plaque volume in ApoE$^{-/-}$ mice. We conclude that inhibiting galectin-3 reduces atherosclerosis.

Results

Lesion quantification

Wild-type C57/Bl6 mice and galectin-3$^{-/-}$ (gal-3$^{-/-}$) mice showed no atherosclerotic lesion development in the aorta or at the bifurcations either following prolonged (>50 weeks) normal chow feeding or after 20 weeks' high-cholesterol feeding. In ApoE$^{-/-}$ mice, atherosclerotic lesions were observed at the bifurcations of the brachiocephalic artery (BA) and at the origins of the left carotid and left subclavian arteries as early as 6 weeks after the start of high-cholesterol feeding with gross changes evident by 12 weeks (Figure 1A). Gross analysis suggested that ApoE$^{-/-}$/gal-3$^{-/-}$ mice had less atherosclerotic lesion formation than ApoE$^{-/-}$ animals (Figure 1A). The absence of galectin-3 resulted in reduced plaque burden in the descending aorta (Figure 1B and C): At 12 weeks, plaque burden (as a percentage of the surface area of the thoracic aorta) was 28 ± 5% in ApoE$^{-/-}$ compared with 12 ± 3% in ApoE$^{-/-}$/gal-3$^{-/-}$ animals, a reduction of 57% ($n = 8$, $P < 0.01$, Figure 1C).

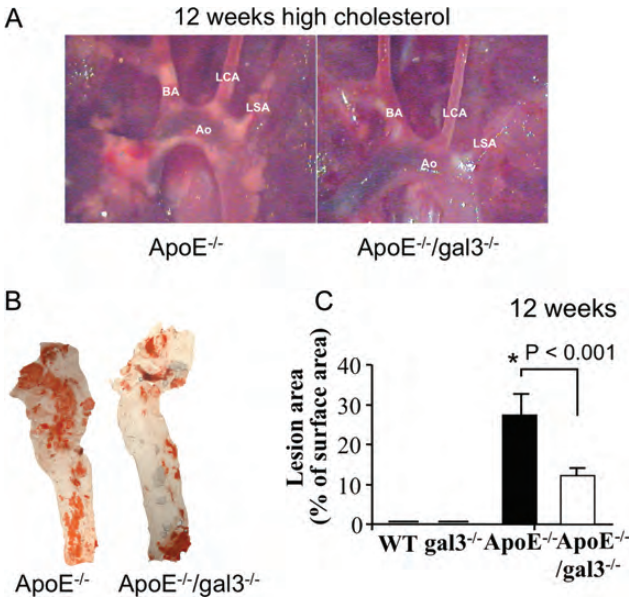

Fig. 1. Deletion of galectin-3 in ApoE$^{-/-}$ mice results in reduced lesion formation. (**A**) Representative images of the aortic arch in situ from ApoE$^{-/-}$ and ApoE$^{-/-}$/ galectin-3$^{-/-}$ (gal3$^{-/-}$) mice following 12 weeks of high-cholesterol feeding. Lesions appeared smaller in the ApoE$^{-/-}$/gal3$^{-/-}$ mice and were not always present at the origins of brachiocephalic artery (BA), left carotid artery (LCA) and left subclavian artery (LSA) (**B**) Representative images of oil red-O-stained descending thoracic aorta from ApoE$^{-/-}$ and ApoE$^{-/-}$/gal3$^{-/-}$ mice showing less lipid accumulation. (**C**) Quantitation of lesion area (oil red-O-staining) in the descending thoracic aorta at 12 weeks by ImageJ (*$P < 0.001$ compared with ApoE$^{-/-}$ mice, $n = 8$). AO, aorta.

Atherosclerotic lesions in the aortic arch were assessed by optical projection tomography (OPT) using our previously validated protocol (Kirkby et al. 2011), which gives a 3-dimensional evaluation of lesion volume in the aortic arch at the origins of the BA and the left carotid and left subclavian arteries. In ApoE$^{-/-}$/galectin-3$^{+/+}$ mice, lesions comprised 12 ± 4.1% of the total lumen volume after 6 weeks on western diet, increasing to 16.5 ± 5.2% after 12 weeks and 57 ± 13% after 20 weeks (Figure 2; $n = 8$, $P < 0.05$). In ApoE$^{-/-}$/gal-3$^{-/-}$ mice, plaque volume was less than that in ApoE$^{-/-}$ mice at all time points tested (8.2 ± 3.1, 9.4 ± 3.2 and 39 ± 11.4% of the total lumen volume at 6, 12 and 20 weeks, respectively; $n = 8$, $P < 0.05$) (Figure 2). Overall, this combined comprehensive analysis indicated that there was ~50% reduction of plaque volume in ApoE$^{-/-}$/gal-3$^{-/-}$ mice.

Plaque structure and composition

Atherosclerotic plaques were not found in the brachiocephalic arteries from mice without the ApoE deletion. Fatty streaks (FS), the initial stage of plaque formation, were observed at 6 weeks in ApoE$^{-/-}$ mice fed western diet, whereas this was negligible in ApoE$^{-/-}$/gal-3$^{-/-}$ mice at this time point (Figure 3). Lesions became larger and more complex after 12 and 20 weeks with the lesion causing almost complete occlusion of the vessel lumen at 20 weeks (Figure 3). In comparison, the plaques in the brachiocephalic arteries of ApoE$^{-/-}$/gal-3$^{-/-}$ mice were significantly smaller (10.5 ± 4.2 vs 32 ± 10.1% at 12 weeks, $P < 0.05$; 40.4 ± 10.2 vs 81.4 ± 19.1% at 20 weeks, $P < 0.05$; Figure 3).

Histological examination of sections of the BA showed dense collagen staining within the plaques of ApoE$^{-/-}$ mice that increased with duration of cholesterol feeding (Figure 4).

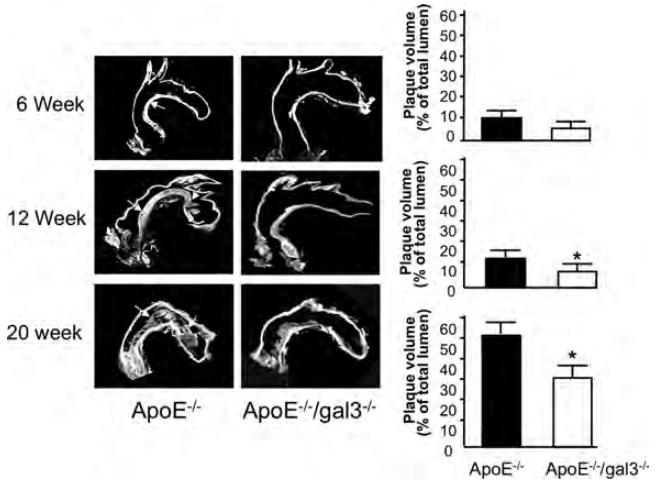

Fig. 2. Galectin-3 deletion results in reduced plaque volume in the aortic arch of ApoE$^{-/-}$ mice as measured by OPT. Mice were fed high-cholesterol diet for 6, 12 and 20 weeks and the aortic arch examined for plaque volume by OPT. Arrows show early lesions in 6-week ApoE$^{-/-}$ mice and more advanced fatty lesions at 12 and 20 weeks. ApoE$^{-/-}$/gal3$^{-/-}$ mice showed little measurable disease at 6 weeks and showed a 35 and a 40% reduction in plaque volume at 12 and 20 weeks, respectively (*$P < 0.05$ compared with ApoE$^{-/-}$, $n = 6$).

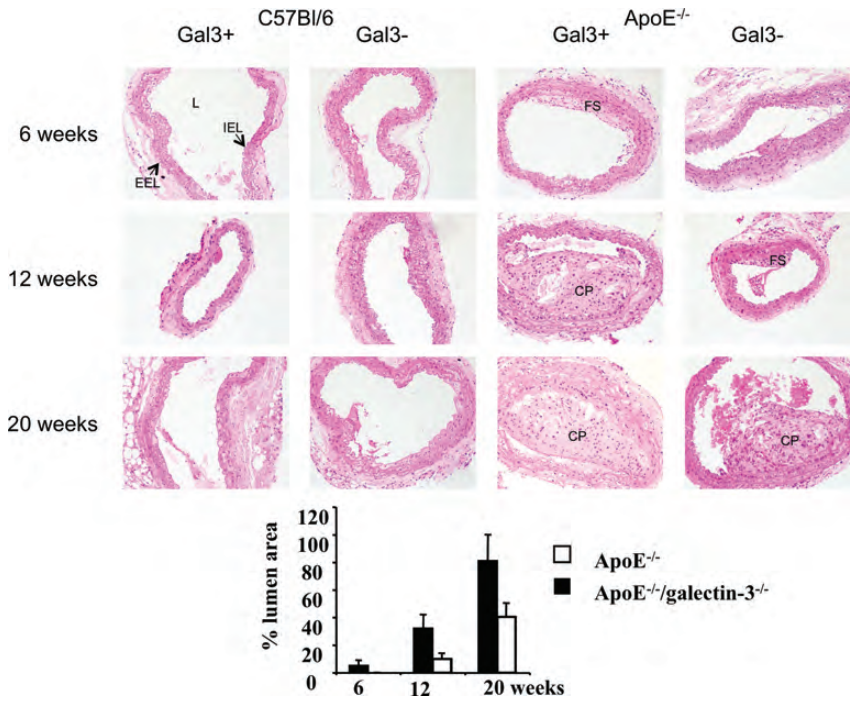

Fig. 3. Sections of the brachiocephalic artery stained with hematoxylin and eosin after 6, 12 and 20 weeks high-cholesterol feeding showing no measurable disease on the luminal (L) surface of the internal elastic lamina (IEL) in wild-type (WT) or gal-3$^{-/-}$ C57/Bl6 mice (left panels). Lesions were evident in ApoE$^{-/-}$ mice (right panels) that developed with time on diet from fatty streak (FS) to more complex plaques (CP). ApoE$^{-/-}$/gal3$^{-/-}$ sections showed smaller and less complex lesions at 12 and 20 weeks (*$P < 0.05$ compared with ApoE$^{-/-}$, $n = 6$). EEL, external elastic lamina.

The brachiocephalic plaques from ApoE$^{-/-}$/gal-3$^{-/-}$ mice had reduced plaque collagen (Figure 4C) and a smaller lipid core (Figure 4D), expressed as a percentage of the total plaque area. Furthermore, there was no evidence for fibrous cap discontinuity or intra-plaque hemorrhage.

Serum lipid profile and bodyweight

Gal-3$^{-/-}$ and WT C57/Bl6 mice showed no difference in body weight when fed normal diet but there was a significant reduction in bodyweight in gal-3$^{-/-}$ mice fed a high-cholesterol diet (Figure 5). In ApoE$^{-/-}$ mice galectin-3 deletion reduced bodyweight in mice fed normal or high-cholesterol diet. Galectin-3 deletion did not affect serum cholesterol. Serum cholesterol concentrations were higher in both ApoE$^{-/-}$ strains (Figure 6A) and increased further following commencement of high-cholesterol feeding. There were no differences in serum cholesterol concentrations between ApoE$^{-/-}$ and ApoE$^{-/-}$/gal-3$^{-/-}$ mice after 6, 12 or 20 weeks (Figure 6A). While there was a trend toward a small decrease in serum triglycerides in and ApoE$^{-/-}$/gal-3$^{-/-}$ compared with ApoE$^{-/-}$ mice, this was significant only at 6 and 20 weeks (analysis of variance (ANOVA) $P < 0.05$). There was no consistent difference in serum free fatty acid concentrations between galectin-3 expressing and null strains (Figure 6B and C).

Macrophage lipoprotein uptake and migration

Bone marrow-derived macrophages (BMDMs) isolated and matured from ApoE$^{-/-}$ and ApoE$^{-/-}$/gal-3$^{-/-}$ mice were used to assess fluorescent di-acetylated LDL uptake in vitro, using flow cytometry. There was no difference in uptake of lipid in F4/80-gated macrophages from ApoE$^{-/-}$/gal-3$^{-/-}$ compared with ApoE$^{-/-}$ mice after either 4 or 48 h treatment with di-acetylated LDL (Figure 6D and E). To assess whether galectin-3 is chemotactic for macrophages, migration of the human monocyte cell line THP1 and mouse BMDMs to recombinant galectin-3 was assessed in a Boyden chamber assay. Human cells migrated toward human galectin-3 with 10 μg/mL being as effective as formyl-methionine-leucine-phenylalanine (fMLP). Similarly, mouse BMDMs migrated toward mouse galectin-3 (Figure 6F). This suggests that galectin-3 may act as a stimulus for monocyte recruitment during plaque progression.

Arginine metabolism

To assess effects on arginine metabolism, iNOS and arginase-1 expression were measured in the left common carotid artery from mice fed a high-cholesterol diet for 6, 12 and 20 weeks. In ApoE$^{-/-}$ mice, there was a predominance of iNOS in early lesions at 6 weeks. Arginase-1 expression increased at 20 weeks accompanied by reduced iNOS expression (Figure 7A and B). In contrast, ApoE$^{-/-}$gal-3$^{-/-}$ arteries showed greater levels of iNOS expression and a 52% reduction in arginase-1 expression at 20 weeks (Figure 7A and -B; $n = 4$ $P < 0.05$), showing that the predominance of arginase-1 in ApoE$^{-/-}$ mice at 20 weeks was reversed in ApoE$^{-/-}$gal-3$^{-/-}$ mice. High arginase-1 expression would suggest that plaque macrophages were polarized to an M2 phenotype. To assess this further, sections of the BA were immunostained for the M2 activation marker chitinase-3-like protein 3 (YM-1) (Figure 7C). The number of YM-1-positive

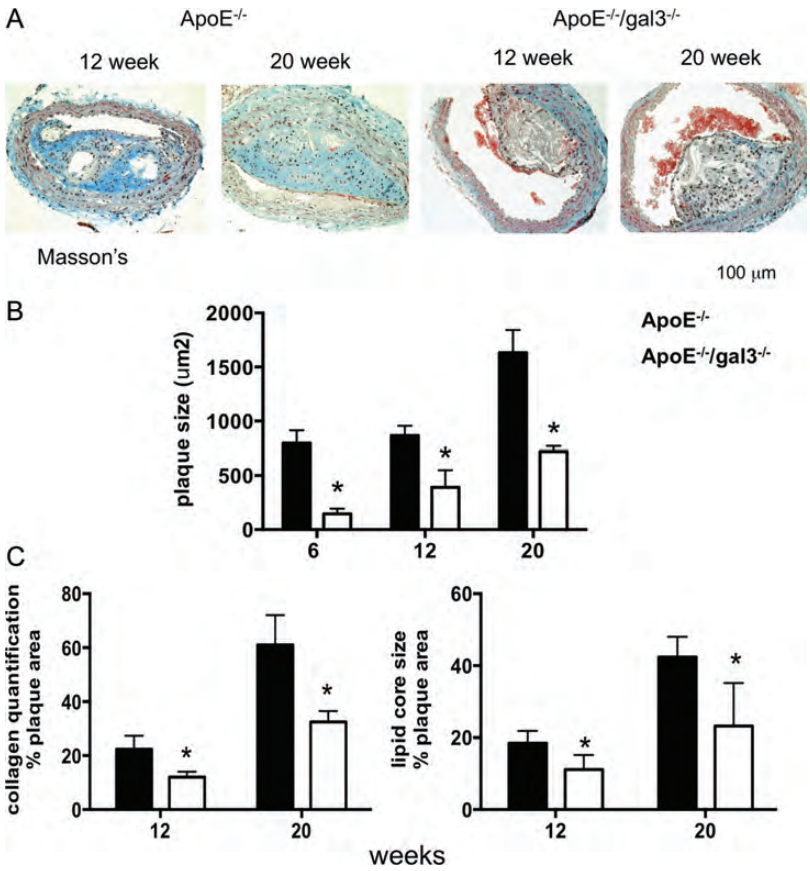

Fig. 4. Galectin-3 deletion results in reduced plaque collagen. Mice were fed high-cholesterol diet for 12 or 20 weeks. Plaque collagen in the brachiocephalic artery was measured by Masson's trichrome. (**A**) Representative sections at 12 and 20 weeks, (**B**) plaque size, (**C**) collagen quantitation showing a reduced percentage of the lesion formed of collagen in gal3$^{-/-}$ mice and (**D**) lipid core size (as a percentage of total plaque area) was also reduced in gal-3$^{-/-}$ mice (*$P < 0.05$, $n = 6$).

macrophages was markedly reduced in ApoE$^{-/-}$gal-3$^{-/-}$ compared with ApoE$^{-/-}$ mice at 20 weeks whether expressed as a percentage of plaque area or as a percentage of total number of plaque foam cells (Figure 7D and E). Dual immunofluorescence staining for the pan-macrophage marker F4/80 and YM-1 showed dual-positive M2 plaque macrophages in ApoE$^{-/-}$ gal-3$^{-/-}$ arteries (Figure 7E).

BMDMs from ApoE$^{-/-}$ and ApoE$^{-/-}$/gal-3$^{-/-}$ mice were treated with IL-4, lipopolysaccharide (LPS) or oxidized LDL to assess M1 and M2 activation by nitrite and arginase activity, respectively. M1 activation in response to LPS or oxidized LDL was not different between BMDMs from the two genotypes (Figure 7F). In contrast, treatment with IL-4 increased arginase activity in ApoE$^{-/-}$ BMDMs, an effect that was abrogated in ApoE$^{-/-}$/gal-3$^{-/-}$ BMDMs (75.1% reduction $n = 4$, $P < 0.01$). Furthermore, oxidized LDL produced a 2.3-fold increase in arginase activation that was reduced by 61% in ApoE$^{-/-}$/gal-3$^{-/-}$ BMDMs (Figure 7G; $n = 4$, $P < 0.05$).

Effect of MCP on plaque volume in vivo

Modified citrus pectin (MCP) is a naturally occurring inhibitor of galectin-3 carbohydrate binding (Glinsky and Raz 2009; Kolatsi-Joannou et al. 2011). To test whether inhibition of galectin-3 in vivo could reduce plaque volume, ApoE$^{-/-}$ mice received western diet for 10 weeks with MCP (1%) in their drinking water for the last 4 weeks. The mice tolerated this regimen well. The descending aorta was examined for disease by oil red-O staining as described in Methods. Administration of MCP produced a 30% reduction in plaque volume in ApoE$^{-/-}$ mice (Figure 8).

Discussion

In this study, we show that ApoE$^{-/-}$ mice deficient in galectin-3 develop smaller plaques with reduced necrotic core and reduced collagen content. An inhibitor of galectin-3 in vivo reduced plaque volume in ApoE$^{-/-}$ mice.

Two previous studies have yielded conflicting results regarding the role of galectin-3 in plaque development. The first study, using C57/Bl6 mice, showed that deletion of galectin-3 increased lesion formation in mice fed a high-fat diet for 8 months (Iacobini et al. 2009). However, high-fat feeding in mice without a defect in lipoprotein metabolism (e.g., ApoE$^{-/-}$ or LDLR$^{-/-}$) does not cause development of advanced lesions and does not induce the same high levels of serum cholesterol. Therefore, this study could not address the role of galectin-3 on the later, and arguably more relevant,

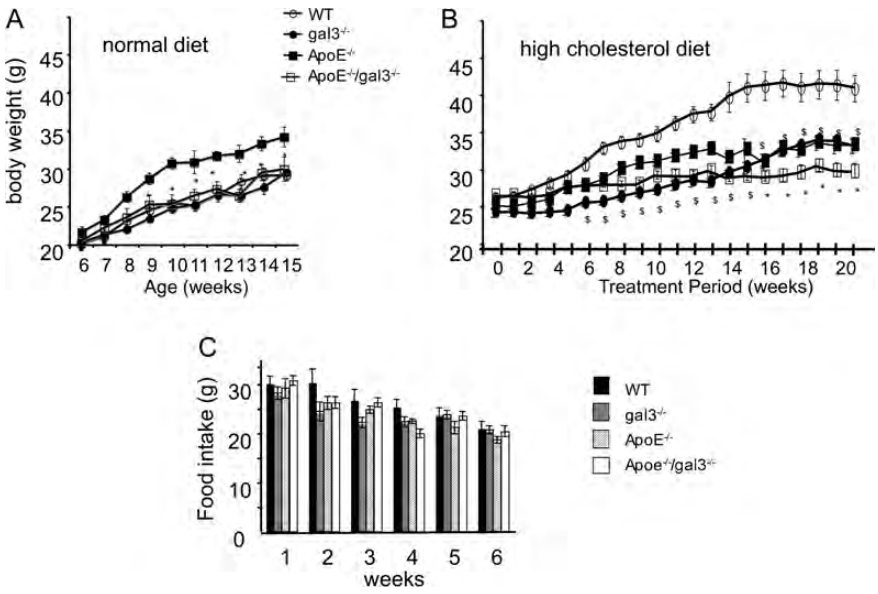

Fig. 5. Galectin-3 deletion results in reduced weight gain with no change in food intake. (**A**) WT, gal3$^{-/-}$, ApoE$^{-/-}$ and ApoE$^{-/-}$/gal3$^{-/-}$ mice were fed normal chow and weight recorded weekly from 6 weeks of age. ApoE$^{-/-}$/gal-3$^{-/-}$ mice gained significantly less weight than ApoE$^{-/-}$ at all time points after 8 weeks of age. Galectin-3 deletion on the C57/Bl6 background had no effect on body weight. (**B**) Mice were fed a high-cholesterol "western" diet commencing at 8 weeks of age for 20 weeks. Galectin-3 deletion on both the C57/Bl6 background and the ApoE$^{-/-}$ background produced a significant reduction in body weight (*$P < 0.05$ compared with ApoE$^{-/-}$, \$ $P < 0.05$ compared with WT, $n = 8$) (**C**) Western diet consumption was not significantly different between the genotypes.

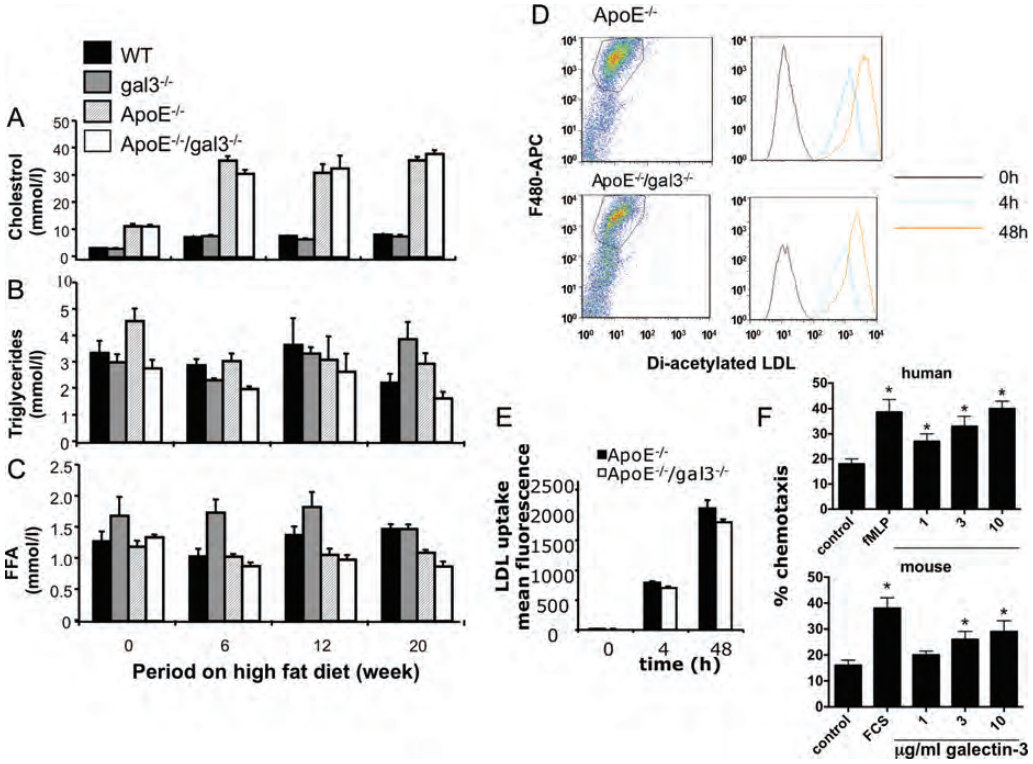

Fig. 6. WT, gal3$^{-/-}$, ApoE$^{-/-}$ and ApoE$^{-/-}$/gal3$^{-/-}$mice were fed western diet commencing at 8 weeks of age and serum obtained at 6, 12 and 20 weeks and analyzed for (**A**) cholesterol (**B**) triglycerides and (**C**) free fatty acids (FFA, $n = 8$). Galectin-3 deletion had no effect on uptake of acetylated LDL by macrophages in vitro. (**D**) BMDMs were exposed to 50 µg/mL di-acetylated LDL for 4 or 48 h. and F4/80 gated macrophages were analyzed by flow cytometry. (**E**) Quantitation of LDL uptake data are mean ± SEM from 4 individual experiments. (**F**) Chemotaxis of human macrophages (top) to human galectin-3 or 10 nM fMLP and mouse BMDMs (bottom) via transwells to recombinant mouse galectin-3 or 10% fetal calf serum (*$P < 0.05$ compared with control wells, $n = 3$).

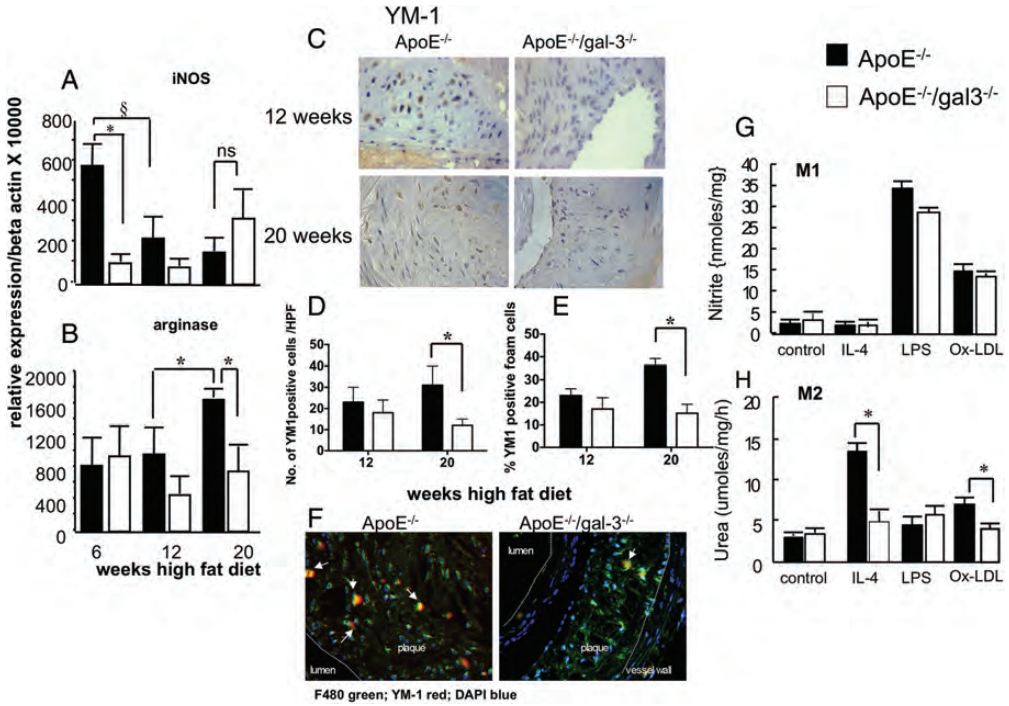

Fig. 7. Galectin-3 deletion reduces arginase-1 activation in arteries in vivo. RNA was isolated from LCA of mice fed a high-cholesterol diet for 6, 12 or 20 weeks and iNOS (**A**) and arginase-1 (**B**) transcript expression measured by qPCR ($n = 5$). Galectin-3$^{-/-}$ mice have reduced M2 plaque macrophages. (**C**) Representative sections of the brachiocephalic artery after 12 and 20 weeks high-cholesterol feeding were stained for the alternative marker YM-1 and quantified by counting positively stained cells within the plaque per high-power field (HPF, **D**) and as a percentage of total foam cells (**E**, $^*P < 0.05$ compared with ApoE$^{-/-}$, $n = 5$). (F) F4/80 (green) and YM-1 (red) staining in brachiocephalic arteries after 20 weeks high-cholesterol feeding. The arrows show dual-positive F480/YM-1 macrophages. BMDMs from ApoE$^{-/-}$ and ApoE$^{-/-}$/gal3$^{-/-}$ mice were treated with 10 ng/mL IL-4, 1 μg/mL LPS or 1 μg/mL oxidized LDL. (**G**) M1 activation was measured by nitrite release. M2 activation (**H**) was measured by arginase assay ($^*P < 0.05$ compared with ApoE$^{-/-}$, $n = 4$).

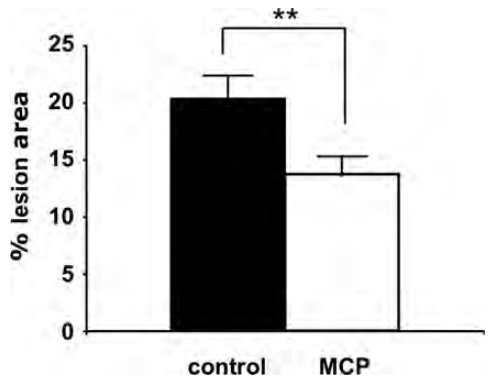

Fig. 8. MCP reduces plaque volume in ApoE$^{-/-}$ mice. ApoE$^{-/-}$ mice were given high-cholesterol diet for 10 weeks and either plain water (control $n = 5$) or 1% MCP ($n = 5$) in the drinking water for the last 4 weeks of high-cholesterol feeding. MCP was freshly prepared and replaced every 2 days. Body weight was recorded during the duration of the study. Plaque volume was determined from oil red-O-staining of the descending aorta and is expressed as a percentage of lumen area.

stages of atherosclerosis. The second study showed that in an atherosclerosis-prone model (ApoE$^{-/-}$ but on a mixed 129sv/C57/Bl6 background), galectin-3 deletion reduced plaque size in older mice (50 weeks) fed a normal diet (Nachtigal et al. 2008). Differences in strain and/or serum cholesterol could be the main factor responsible for this paradox.

The reduced plaque burden was not due to reduced serum cholesterol as this was not different between genotypes. There was a small reduction in triglycerides in ApoE$^{-/-}$/gal-3$^{-/-}$ mice; however, the significance of this finding in relation to plaque burden requires further study. Galectin-3 deletion had no effect on macrophage uptake of modified LDL in vitro, suggesting that differential uptake of lipid is not a major mechanism contributing to the differences we see on plaque progression in vivo. However, we did observe reduced weight gain despite similar fat ingestion in gal-3$^{-/-}$ mice. At present, the mechanism of this reduced weight gain is unclear but it may be due to a previously described function of galectin-3 to stimulate adipocyte proliferation (Kiwaki et al. 2007). Indeed, high levels of circulating galectin-3 have been associated with obesity (Weigert et al. 2010). The fact that the difference in weight gain was much less apparent when C57Bl/6 mice were fed a normal diet could suggest that high serum cholesterol may provide a stimulus for galectin-3 release which could affect adipocytes indirectly.

Previous studies have shown that early events in atherosclerosis are Th1 dominated, as IL-12 and tumor necrosis factor-α (TNFα) are predominately expressed in early atheromatous lesions (Frostegard et al. 1999; Davenport and Tipping 2003) and deficiency of inducible nitric oxide synthase (iNOS) (Miyoshi et al. 2006) or interferon γ (Vats et al. 2006) shows reduced plaque burden in atherosclerosis-prone mice. However, later stages of atherosclerosis are associated

with a switch to a Th2-dominant response that is largely anti-inflammatory (Zhou et al. 1998; Mallat, Besnard et al. 1999; Mallat, Heymes et al. 1999; Davenport and Tipping 2003). Our study confirms these findings and demonstrates a switch in arginine metabolizing enzymes during disease progression, with iNOS expressed in early (6 weeks) lesions and arginase-1 expression increased in later (20 weeks) lesions. We suggest that this switch is essential for plaque progression and that a failure or reversal of this switch, as observed in galectin-3-deficient mice, results in reduced plaque burden. This switch in arginine metabolism from iNOS to arginase-1 could be considered profibrotic (Hesse et al. 2001) as arginase-1 up-regulates several genes involved in fibrosis (Liu et al. 2004; Wynn 2004; Fichtner-Feigl et al. 2006) such as fibronectin and other matrix proteins (Doucet et al. 1998; Rishikof et al. 2002; Herbert et al. 2004) and induces fibroblast proliferation, which would tend to favor fibrous cap formation and plaque stability. However, other studies have shown that specific deletion of arginase-1 in macrophages actually promotes fibrosis, at least in a model of schistosomiasis (Pesce et al. 2009). In addition, although it has been suggested that the Th2 cytokine IL-13 improves the stability of established plaques (Cardilo-Reis et al. 2012), another study showed IL-4 to be proatherogenic (Davenport and Tipping 2003) so the role of macrophage derived arginase-1 in the development of fibrosis is not clear.

We have previously shown that galectin-3$^{-/-}$ macrophages have a specific defect in M2 alternative macrophage activation (MacKinnon et al. 2008). In our present study, we show that the iNOS-to-arginase-1 switch is reversed in galectin-3$^{-/-}$ mice. There was significantly reduced iNOS in lesions at 6 weeks and reduced arginase-1 in later lesions at 20 weeks resulting in smaller plaques. This was accompanied by a decrease in the number of YM-1-positive, M2 macrophages in advanced plaques of gal-3$^{-/-}$ mice. In vitro oxidized LDL increased NO and arginase-1 activity, suggesting that serum phospholipids can affect macrophage heterogeneity (Gordon 2007). However, galectin-3 deletion reduced oxidized LDL-induced arginase-1 activity without affecting NO release, which could suggest additional affects of galectin-3 under conditions of high circulating cholesterol and could further explain the different effect of galectin-3 deletion in mice with normal cholesterol metabolism.

In humans, M2 macrophages predominate in diseased vs normal intima of carotid arteries, and patients with a predisposition toward an M2 phenotype may be more susceptible to atherosclerotic disease (Waldo et al. 2008). However, the function of these M2 plaque macrophages is still unknown. Moreover, additional subsets of macrophages reside within the lipid core vs the stable cell-rich area of human carotid plaques (Bouhlel et al. 2007) which differentially regulate cholesterol efflux (Chinetti-Gbaguidi et al. 2011). Therefore, although it may be over simplistic to implicate a single macrophage phenotype in the pathogenesis of atherosclerosis, our studies show galectin-3 deletion results in reduced M2 polarization within plaques accompanied by reduced disease in atherosclerosis-prone mice.

Galectin-3 is known to be a chemoattractant for monocytes and macrophages (Sano et al. 2000). Therefore, it is possible that galectin-3 may facilitate plaque progression by augmenting monocyte recruitment. We show that galectin-3 stimulates human and mouse monocyte/macrophage chemotaxis in vitro. However, further in vivo studies are required to assess whether galectin-3 affects plaque monocyte recruitment/egress.

Our studies show that when galectin-3 is deleted from the outset there is reduced plaque formation despite high serum cholesterol, and we would predict that strategies to block galectin-3 function may be advantageous in inhibiting plaque formation without adversely affecting plaque stability. To determine whether inhibiting galectin-3 function in established plaques could reduce plaque burden, we used modified citrus pectin (MCP), which is a naturally occurring pectin found in the peel and pulp of citrus fruits. In the United States, MCP is registered as a food supplement and is generally regarded as safe. MCP inhibits galectin-3 binding and function in vitro and in vivo (Pienta et al. 1995; Nangia-Makker et al. 2002; Liu et al. 2008; Glinsky and Raz 2009). Recent evidence shows that MCP reduces renal fibrosis in vivo (Kolatsi-Joannou et al. 2011) and is being developed as an anti-cancer agent for prostate cancer (Guess et al. 2003). We show that administration of 1% MCP in the drinking water to ApoE$^{-/-}$ mice for 4 weeks at the end of a 10-week high-cholesterol feeding regimen reduced plaque burden in the descending aorta compared with vehicle control. As MCP is a relatively nonspecific galectin-3 inhibitor, it is possible that it could reduce lesion size by off-target effects. This point will be clarified in future investigations by determining whether MCP inhibits lesion formation in galectin-3-deficient mice and by the use of more selective inhibitors.

In summary, we show that mice deficient in galectin-3 display a reversal of the iNOS to arginase switch within plaques, reduced M2 activation of plaque macrophages and reduced atherosclerosis in vivo. We have previously demonstrated that galectin-3 inhibitors reduce M2 alternative macrophage activation (MacKinnon et al. 2008, 2012). Strategies to inhibit galectin-3 function may reduce plaque progression and potentially represent a novel therapeutic strategy in the treatment of atherosclerotic disease.

Materials and methods

Animals and treatments

Gal-3$^{-/-}$ C57/Bl6 mice generated by gene-targeting technology (Hsu et al. 2000) were used to generate ApoE-deficient/galectin-3-deficient mice. C57/Bl6 mice and ApoE-deficient C57/Bl6 mice (ApoE$^{-/-}$) were obtained from Harlan (UK). Double-knockout (ApoE- and galectin-3-deficient) mice (ApoE$^{-/-}$gal-3$^{-/-}$) were generated by F1 intercross. ApoE$^{-/-}$/gal-3$^{+/+}$ littermates were used as comparison. All the mice were given free access to water and standard commercial mouse diet (Special Diet Services, Witham, Essex, UK), and maintained under a 12 h light/dark cycle. From age 10–12 weeks, the mice were given western diet containing 21% milk fat and 0.15% cholesterol (Research Diets, Inc., New Brunswick, NJ), for 6, 12 or 20 weeks. Body weight and food intake were recorded weekly. At various timepoints, 6–8 mice from each strain were euthanized by terminal anesthesia, and blood samples were obtained from the right ventricle. The

mice were then perfusion fixed with Methyl Carnoy's solution (6 methanol: 3 chloroform: 1 acetic acid) through cardiac puncture. The entire aortic tree including the heart was dissected free of fat and other tissues, and fixed in Methyl Carnoy's fixative solution. MCP was purchased from Allergy Research Group (allergyresearchgroup.com) and prepared as a 1% solution in the drinking water and replaced every 2 days. Analyses were performed by an operator blinded to origin of the samples.

Assessment of atherosclerotic lesions

Lipid-rich atherosclerotic plaques of the entire descending thoracic aorta were stained with oil red-O as per the manufacturer's instructions and plaque coverage of the intimal surface was calculated as a percentage of the total vessel surface area using ImageJ.

Quantification of lesions in the aortic arch was achieved using optical projection tomography (OPT), as described (Kirkby et al. 2011). This method allows calculation of a volume for the entire lesion. Briefly, aortic arches were isolated and embedded in 1.5% low melting point agarose (Invitrogen, UK), dehydrated in methanol (100%; 24 h) and optically cleared in benzyl alcohol:benzyl benzoate (1:2 v/v; 24 h). Images were generated using a Bioptonics 3001 OPT tomograph. Studies used emission imaging, after UV illumination (425 nm excitation filter with 40 nm band pass; 475 nm long passemission filter; 1.048 Mpixel scanning resolution). Magnification was chosen to provide the smallest voxel size that allowed imaging of the whole region of interest. Raw data (400 projections per scan at 0.9° increments) were subjected to Hamming-filtered back-projection using the NRecon software (Skyscan, Belgium). Quantification was performed using the CTan software (Skyscan). Briefly, lesion and lumen volumes were segmented by semi-automated tracing of the internal elastic lamina and subsequent gray-level thresholding to distinguish atheroma from lumen. The lesion volume was presented as a percentage of the total area within the internal elastic lamina.

Histology. The brachiocephalic trunk was fixed in Methyl Carnoy's solution, embedded in paraffin and 6-μm-thick sections, taken from the bifurcation, were stained with Harris hematoxylin and eosin (H&E) for histological analysis and Masson's trichrome for collagen fiber analysis (Deuchar et al. 2011). Lipid (or necrotic) core was positively identified as intra-plaque areas showing no staining in Masson's stained sections, as these are regarded as areas previously containing lipids before the fixing procedure (Johnson et al. 2005). Positively identified areas were measured by color deconvolution using Photoshop CS6. For immunohistochemistry, the following primary antibodies were used: Rat anti-mouse F4/80 clone CI: A3-1 (Serotec, Oxford, UK) and rabbit anti-YM-1 (stem cell technologies). Following labeling with secondary, biotinylated, species–specific antibodies (Dako), positive staining was visualized using Vectastain Elite RTU reagent and liquid diaminobenzamine (DAB). Sections were counterstained with Mayer's hematoxylin and mounted with pertex. To assess macrophage infiltration (F4/80-positive cells) and alternative macrophages (YM-1 positive cells), digital images of the sections were captured using the openlab software. Nonoverlapping fields at ×400 magnification were analyzed in a blinded fashion. Data were expressed as the mean score ±SE per 5 high power fields. YM-1-positive cells were counted as total number of YM-1-positive cells per plaque and as a percentage of the number of foam cells. For dual immunofluorescence studies, sections were labeled with F4/80 followed by horseradish peroxidase-labeled goat anti-rat IgG (Dako) and tyramide green reagent, as per the manufacturer's instructions (Perkin Elmer). Then, following 10 min microwaving with 10 mM citrate (pH 6.0), slides were incubated sequentially with rabbit anti-YM-1 and donkey anti-rabbit Alexa 555 (Life Technologies, UK). Slides were mounted in Fluoromount-G.

Blood lipid profile

Serum cholesterol, triglycerides and free fatty acids were measured by standard enzymatic colorimetric assay kits from Alpha Laboratories, UK.

Cell culture. THP-1 cells were obtained from the American Tissue Culture Collection (Rockville, MD) and maintained in RPMI 1640 medium supplemented with 10% fetal bovine serum (FBS). Cells were differentiated with 100 ng/mL PMA for 24 h.

Preparation of BMDMs. Mouse bone marrow-derived macrophages (BMDMs) were prepared by flushing femurs and tibias and maturing resulting bone marrow cells in Dulbecco's modified Eagle's medium (DMEM) containing 10% FBS and 20% L929 conditioned media for 7–9 days (MacKinnon et al. 2008).

Uptake of acetylated LDL. BMDMs were serum starved for 24 h and then incubated in DMEM containing 50 μg/mL acetylated LDL labeled with 1,1′-dioctadecyl-3,3,3′,3′-tetramethylindocarbocyanine perchlorate (Dio-AC-LDL; Bioquote Limited, UK) for 4 or 48 h. The cells were washed with phosphate buffered saline and stained with allophycocyanin (APC)–labeled F4/80 monoclonal antibody (AbD Serotec, UK) for 30 min and analyzed by flow cytometry (Facscaliber, Becton Dickinson, Oxford, UK).

Chemotaxis assay. BMDMs or the human macrophage cell line THP1 were seeded into the upper chambers of 8 μm pore size modified Boyden chambers as per the manufacturer's instructions (CytoSelect 24-well migration assay, Cambridge Biosciences, UK). Recombinant human or mouse galectin-3 (R&D Systems, UK) or 10 nM *N*-fMLP was added to the lower chamber and cells were allowed to migrate for 2 h at 37°C. Cells remaining in the upper chamber were wiped with a cotton tip and cells attached to the underside of the membrane were fixed and stained and eluted as per the manufacturer's instructions. Chemotaxis is expressed as a percentage of an unwiped control.

Assessment of macrophage phenotype

BMDMs were polarized to an M1 or M2 phenotype by treatment of serum-starved BMDMs for 24 h with 1 μg/mL lipopolysaccharide (M1) or 10 ng/mL IL-4 (M2). M1 activation

was measured by nitrite release using the Griess reaction (Sigma-Aldrich, UK). M2 activation was measured by arginase activity assessed by the production of urea generated by the arginase-dependent hydrolysis of L-arginine as previously described (MacKinnon et al. 2008).

Transcript analysis

Total RNA from cultured macrophages and the left common carotid artery was extracted using an RNeasy kit (Quiagen) and reverse transcribed into cDNA using random hexamers (Applied Biosystems). A SYBR green-based quantitative fluorescence method (Applied Biosystems) was used for analysis of gene expression (MacKinnon et al. 2008). The following primers were used: Mouse β-actin: Forward 5′-AG AGGGAAATCGTGCGTGAC-3′, reverse5′-CAATAGTGATG ACCTGGCCGT-3′, mouse arginase-1: Forward 5′-TTGGGT GGATGCTCACACTG-3′, reverse 5′-TTGCCCATGCAGATT CCC-3′; mouse iNOS: Forward 5′-CAGCTGGGCTGTACAA ACCTT-3′, reverse 5′-CATTGGAAGTGAAGCGTTTCG-3′.

The data were expressed as mean ± SE of the mean. Statistical significance was evaluated by one-way ANOVA followed by the Student–Newman–Keuls test for multiple comparisons. *P*-value <0.05 was considered significant.

Funding

This work was supported by the Wellcome Trust UK and the British Heart Foundation.

Acknowledgements

We thank Kirsten Atkinson for expert technical assistance.

Conflict of interest

None declared.

Abbreviations

ANOVA, analysis of variance; APC, allophycocyanin; ApoE$^{-/-}$, apolipoprotein E-deficient; BA, brachiocephalic artery; BMDMs, bone marrow-derived macrophages; CVD, cardiovascular disease; FBS, fetal bovine serum; FS, fatty streaks; iNOS, inducible nitric oxide; LCA, left carotid artery; LDL, low-density lipoprotein; MCP, modified citrus pectin; PBS, phosphate buffered saline; SE, standard error; TNFα, tumor necrosis factor-α.

References

Arar C, Gaudin JC, Capron L, Legrand A. 1998. Galectin-3 gene (LGALS3) expression in experimental atherosclerosis and cultured smooth muscle cells. *FEBS Lett*. 430:307–311.

Bouhlel MA, Derudas B, Rigamonti E, Dievart R, Brozek J, Haulon S, Zawadzki C, Jude B, Torpier G, Marx N, et al. 2007. PPARgamma activation primes human monocytes into alternative M2 macrophages with anti-inflammatory properties. *Cell Metab*. 6:137–143.

Cardilo-Reis L, Gruber S, Schreier SM, Drechsler M, Papac-Milicevic N, Weber C, Wagner O, Stangl H, Soehnlein O, Binder CJ. 2012. Interleukin-13 protects from atherosclerosis and modulates plaque composition by skewing the macrophage phenotype. *EMBO Mol Med*. 4:1072–1086.

Chinetti-Gbaguidi G, Baron M, Bouhlel MA, Vanhoutte J, Copin C, Sebti Y, Derudas B, Mayi T, Bories G, Tailleux A, et al. 2011. Human atherosclerotic plaque alternative macrophages display low cholesterol handling but high phagocytosis because of distinct activities of the PPAR{gamma} and LXR{alpha} Pathways. *Circ Res*. 108:985–995.

Davenport P, Tipping PG. 2003. The role of interleukin-4 and interleukin-12 in the progression of atherosclerosis in apolipoprotein E-deficient mice. *Am J Pathol*. 163:1117–1125.

de Boer RA, van Veldhuisen DJ, Gansevoort RT, Muller Kobold AC, van Gilst WH, Hillege HL, Bakker SJ, van der Harst P. 2012. The fibrosis marker galectin-3 and outcome in the general population. *J Intern Med*.

Deuchar GA, McLean D, Hadoke PW, Brownstein DG, Webb DJ, Mullins JJ, Chapman K, Seckl JR, Kotelevtsev YV. 2011. 11beta-hydroxysteroid dehydrogenase type 2 deficiency accelerates atherogenesis and causes proinflammatory changes in the endothelium in apoe-/- mice. *Endocrinology*. 152:236–246.

Dong S, Hughes RC. 1997. Macrophage surface glycoproteins binding to galectin-3 (Mac-2-antigen). *Glycoconj J*. 14:267–274.

Doucet C, Brouty-Boye D, Pottin-Clemenceau C, Jasmin C, Canonica GW, Azzarone B. 1998. IL-4 and IL-13 specifically increase adhesion molecule and inflammatory cytokine expression in human lung fibroblasts. *Int Immunol*. 10:1421–1433.

Dumic J, Dabelic S, Flogel M. 2006. Galectin-3: An open-ended story. *Biochim Biophys Acta*. 1760:616–635.

Fichtner-Feigl S, Strober W, Kawakami K, Puri RK, Kitani A. 2006. IL-13 signaling through the IL-13alpha2 receptor is involved in induction of TGF-beta1 production and fibrosis. *Nat Med*. 12:99–106.

Frostegard J, Ulfgren AK, Nyberg P, Hedin U, Swedenborg J, Andersson U, Hansson GK. 1999. Cytokine expression in advanced human atherosclerotic plaques: Dominance of pro-inflammatory (Th1) and macrophage-stimulating cytokines. *Atherosclerosis*. 145:33–43.

Glinsky VV, Raz A. 2009. Modified citrus pectin anti-metastatic properties: One bullet, multiple targets. *Carbohydr Res*. 344:1788–1791.

Gordon S. 2007. Macrophage heterogeneity and tissue lipids. *J Clin Invest*. 117:89–93.

Guess BW, Scholz MC, Strum SB, Lam RY, Johnson HJ, Jennrich RI. 2003. Modified citrus pectin (MCP) increases the prostate-specific antigen doubling time in men with prostate cancer: A phase II pilot study. *Prostate Cancer Prostatic Dis*. 6:301–304.

Gullestad L, Ueland T, Kjekshus J, Nymo SH, Hulthe J, Muntendam P, Adourian A, Bohm M, van Veldhuisen DJ, Komajda M, et al. 2012. Galectin-3 predicts response to statin therapy in the Controlled Rosuvastatin Multinational Trial in Heart Failure (CORONA). *Eur Heart J*. 18:2290–2296.

Hansson GK, Robertson AK, Soderberg-Naucler C. 2006. Inflammation and atherosclerosis. *Annu Rev Pathol*. 1:297–329.

Henderson NC, Mackinnon AC, Farnworth SL, Poirier F, Russo FP, Iredale JP, Haslett C, Simpson KJ, Sethi T. 2006. Galectin-3 regulates myofibroblast activation and hepatic fibrosis. *Proc Natl Acad Sci USA*. 103:5060–5065.

Herbert DR, Holscher C, Mohrs M, Arendse B, Schwegmann A, Radwanska M, Leeto M, Kirsch R, Hall P, Mossmann H, et al. 2004. Alternative macrophage activation is essential for survival during schistosomiasis and downmodulates T helper 1 responses and immunopathology. *Immunity*. 20:623–635.

Hesse M, Modolell M, La Flamme AC, Schito M, Fuentes JM, Cheever AW, Pearce EJ, Wynn TA. 2001. Differential regulation of nitric oxide synthase-2 and arginase-1 by type 1/type 2 cytokines in vivo: Granulomatous pathology is shaped by the pattern of L-arginine metabolism. *J Immunol*. 167:6533–6544.

Ho JE, Liu C, Lyass A, Courchesne P, Pencina MJ, Vasan RS, Larson MG, Levy D. 2012. Galectin-3, a marker of cardiac fibrosis, predicts incident heart failure in the community. *J Am Coll Cardiol*. 60:1249–1256.

Hsu DK, Yang RY, Pan Z, Yu L, Salomon DR, Fung-Leung WP, Liu FT. 2000. Targeted disruption of the galectin-3 gene results in attenuated peritoneal inflammatory responses. *Am J Pathol*. 156:1073–1083.

Iacobini C, Menini S, Ricci C, Scipioni A, Sansoni V, Cordone S, Taurino M, Serino M, Marano G, Federici M, et al. 2009. Accelerated lipid-induced atherogenesis in galectin-3-deficient mice: Role of lipoxidation via receptor-mediated mechanisms. *Arterioscler Thromb Vasc Biol*. 29:831–836.

Johnson J, Carson K, Williams H, Karanam S, Newby A, Angelini G, George S, Jackson C. 2005. Plaque rupture after short periods of fat feeding in the

apolipoprotein E-knockout mouse: Model characterization and effects of pravastatin treatment. *Circulation*. 111:1422–1430.

Kirkby NS, Low L, Seckl JR, Walker BR, Webb DJ, Hadoke PW. 2011. Quantitative 3-dimensional imaging of murine neointimal and atherosclerotic lesions by optical projection tomography. *PLoS One*. 6:e16906.

Kiwaki K, Novak CM, Hsu DK, Liu FT, Levine JA. 2007. Galectin-3 stimulates preadipocyte proliferation and is up-regulated in growing adipose tissue. *Obesity (Silver Spring)*. 15:32–39.

Kolatsi-Joannou M, Price KL, Winyard PJ, Long DA. 2011. Modified citrus pectin reduces galectin-3 expression and disease severity in experimental acute kidney injury. *PLoS One*. 6:e18683.

Liu HY, Huang ZL, Yang GH, Lu WQ, Yu NR. 2008. Inhibitory effect of modified citrus pectin on liver metastases in a mouse colon cancer model. *World J Gastroenterol*. 14:7386–7391.

Liu T, Jin H, Ullenbruch M, Hu B, Hashimoto N, Moore B, McKenzie A, Lukacs NW, Phan SH. 2004. Regulation of found in inflammatory zone 1 expression in bleomycin-induced lung fibrosis: Role of IL-4/IL-13 and mediation via STAT-6. *J Immunol*. 173:3425–3431.

MacKinnon AC, Farnworth SL, Hodkinson PS, Henderson NC, Atkinson KM, Leffler H, Nilsson UJ, Haslett C, Forbes SJ, Sethi T. 2008. Regulation of alternative macrophage activation by galectin-3. *J Immunol*. 180:2650–2658.

Mackinnon AC, Gibbons MA, Farnworth SL, Leffler H, Nilsson UJ, Delaine T, Simpson AJ, Forbes SJ, Hirani N, Gauldie J, et al. 2012. Regulation of TGF-beta1 driven lung fibrosis by galectin-3. *Am J Respir Crit Care Med*. 185:537–546.

Maeda N, Kawada N, Seki S, Ikeda K, Okuyama H, Hirabayashi J, Kasai KI, Yoshizato K. 2004. Involvement of galectin-1 and galectin-3 in proliferation and migration of rat hepatic stellate cells in culture. *Comp Hepatol*. 3 Suppl 1:S10.

Mallat Z, Besnard S, Duriez M, Deleuze V, Emmanuel F, Bureau MF, Soubrier F, Esposito B, Duez H, Fievet C, et al. 1999. Protective role of interleukin-10 in atherosclerosis. *Circ Res*. 85:e17–e24.

Mallat Z, Heymes C, Ohan J, Faggin E, Leseche G, Tedgui A. 1999. Expression of interleukin-10 in advanced human atherosclerotic plaques: Relation to inducible nitric oxide synthase expression and cell death. *Arterioscler Thromb Vasc Biol*. 19:611–616.

Miyoshi T, Li Y, Shih DM, Wang X, Laubach VE, Matsumoto AH, Helm GA, Lusis AJ, Shi W. 2006. Deficiency of inducible NO synthase reduces advanced but not early atherosclerosis in apolipoprotein E-deficient mice. *Life Sci*. 79:525–531.

Nachtigal M, Al-Assaad Z, Mayer EP, Kim K, Monsigny M. 1998. Galectin-3 expression in human atherosclerotic lesions. *Am J Pathol*. 152:1199–1208.

Nachtigal M, Ghaffar A, Mayer EP. 2008. Galectin-3 gene inactivation reduces atherosclerotic lesions and adventitial inflammation in ApoE-deficient mice. *Am J Pathol*. 172:247–255.

Nakahara S, Oka N, Raz A. 2005. On the role of galectin-3 in cancer apoptosis. *Apoptosis*. 10:267–275.

Nangia-Makker P, Hogan V, Honjo Y, Baccarini S, Tait L, Bresalier R, Raz A. 2002. Inhibition of human cancer cell growth and metastasis in nude mice by oral intake of modified citrus pectin. *J Natl Cancer Inst*. 94: 1854–1862.

Pesce JT, Ramalingam TR, Mentink-Kane MM, Wilson MS, El Kasmi KC, Smith AM, Thompson RW, Cheever AW, Murray PJ, Wynn TA. 2009. Arginase-1-expressing macrophages suppress Th2 cytokine-driven inflammation and fibrosis. *PLoS Pathog*. 5:e1000371.

Pienta KJ, Naik H, Akhtar A, Yamazaki K, Replogle TS, Lehr J, Donat TL, Tait L, Hogan V, Raz A. 1995. Inhibition of spontaneous metastasis in a rat prostate cancer model by oral administration of modified citrus pectin. *J Natl Cancer Inst*. 87:348–353.

Rishikof DC, Ricupero DA, Kuang PP, Liu H, Goldstein RH. 2002. Interleukin-4 regulates connective tissue growth factor expression in human lung fibroblasts. *J Cell Biochem*. 85:496–504.

Roger VL, Go AS, Lloyd-Jones DM, Adams RJ, Berry JD, Brown TM, Carnethon MR, Dai S, de Simone G, Ford ES, et al. 2011. Heart disease and stroke statistics–2011 update: A report from the American Heart Association. *Circulation*. 123:e18–e209.

Sano H, Hsu DK, Yu L, Apgar JR, Kuwabara I, Yamanaka T, Hirashima M, Liu FT. 2000. Human galectin-3 is a novel chemoattractant for monocytes and macrophages. *J Immunol.* 165:2156–2164.

Sharma UC, Pokharel S, van Brakel TJ, van Berlo JH, Cleutjens JP, Schroen B, Andre S, Crijns HJ, Gabius HJ, Maessen J, et al. 2004. Galectin-3 marks activated macrophages in failure-prone hypertrophied hearts and contributes to cardiac dysfunction. *Circulation*. 110:3121–3128.

Tsai TH, Sung PH, Chang LT, Sun CK, Yeh KH, Chung SY, Chua S, Chen YL, Wu CJ, Chang HW, et al. 2012. Value and level of galectin-3 in acute myocardial infarction patients undergoing primary percutaneous coronary intervention. *J Atheroscler Thromb*. 19:1073–1082.

Vats D, Mukundan L, Odegaard JI, Zhang L, Smith KL, Morel CR, Wagner RA, Greaves DR, Murray PJ, Chawla A. 2006. Oxidative metabolism and PGC-1beta attenuate macrophage-mediated inflammation. *Cell Metab*. 4:13–24.

Waldo SW, Li Y, Buono C, Zhao B, Billings EM, Chang J, Kruth HS. 2008. Heterogeneity of human macrophages in culture and in atherosclerotic plaques. *Am J Pathol*. 172:1112–1126.

Weigert J, Neumeier M, Wanninger J, Bauer S, Farkas S, Scherer MN, Schnitzbauer A, Schaffler A, Aslanidis C, Scholmerich J, et al. 2010. Serum galectin-3 is elevated in obesity and negatively correlates with glycosylated hemoglobin in type 2 diabetes. *J Clin Endocrinol Metab*. 95:1404–1411.

Wynn TA. 2004. Fibrotic disease and the T(H)1/T(H)2 paradigm. *Nat Rev Immunol*. 4:583–594.

Zhou X, Paulsson G, Stemme S, Hansson GK. 1998. Hypercholesterolemia is associated with a T helper (Th) 1/Th2 switch of the autoimmune response in atherosclerotic apo E-knockout mice. *J Clin Invest*. 101: 1717–1725.